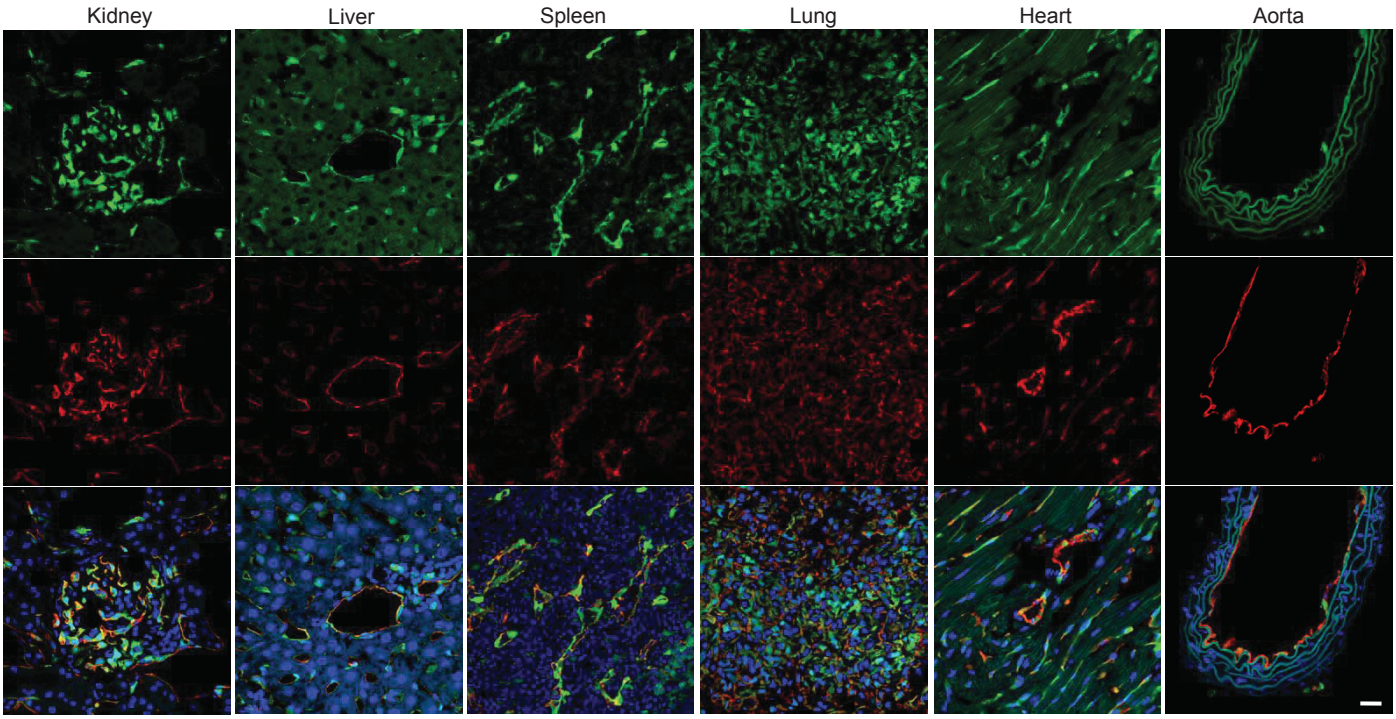

Figure S1. Confirmation of the pan-endothelial-specific pattern of Cre recombinase expression in *Tek*-Cre mice. Cre recombinase expression in *Tek*-Cre mice was assessed by immunostaining with PECAM1 (red) on sections containing kidney, liver, spleen, lung, heart, and aorta tissues from 8-week-old *Tek*-Cre^{+};EGFP-ChAT mice. Sections were counterstained with DAPI (blue). Bar: 20 μm.

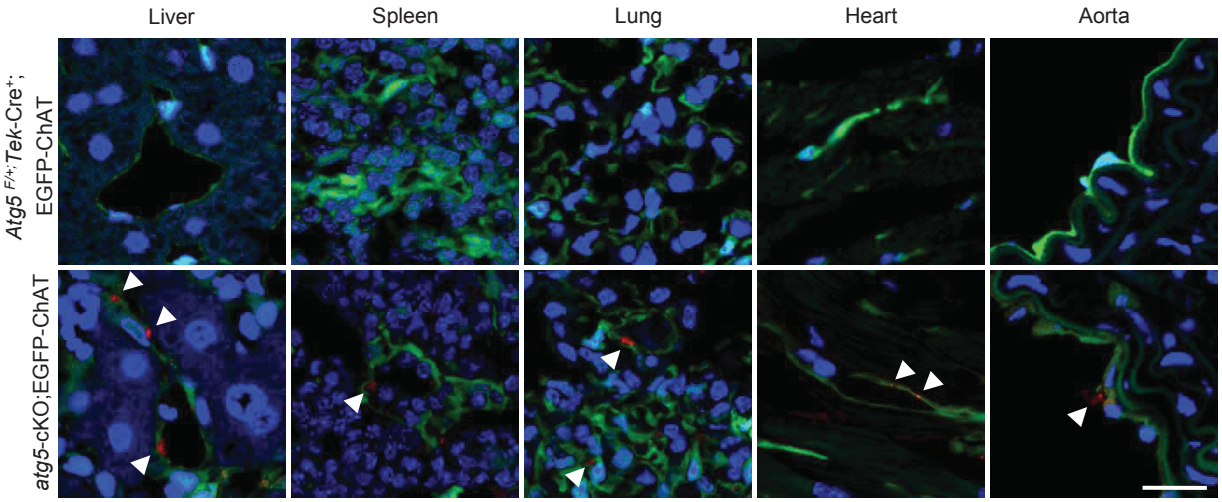

Figure S2. SQSTM1 accumulation in the ECs of *atg5*-cKO mice. Representative images of immunofluorescence analysis using 8-week-old *Atg5*$^{F/+}$;*Tek*-Cre^{+};EGFP-ChAT (upper) and *atg5*-cKO;EGFP-ChAT (lower) mice. Sections containing liver, spleen, lung, heart, and aorta tissues were immunostained for SQSTM1 (red) and for DAPI (blue) as counterstaining. Arrowheads indicate SQSTM1-positive aggregates localized in EGFP-positive ECs of *atg5*-cKO;EGFP-ChAT mice. Bar: 20 μm.

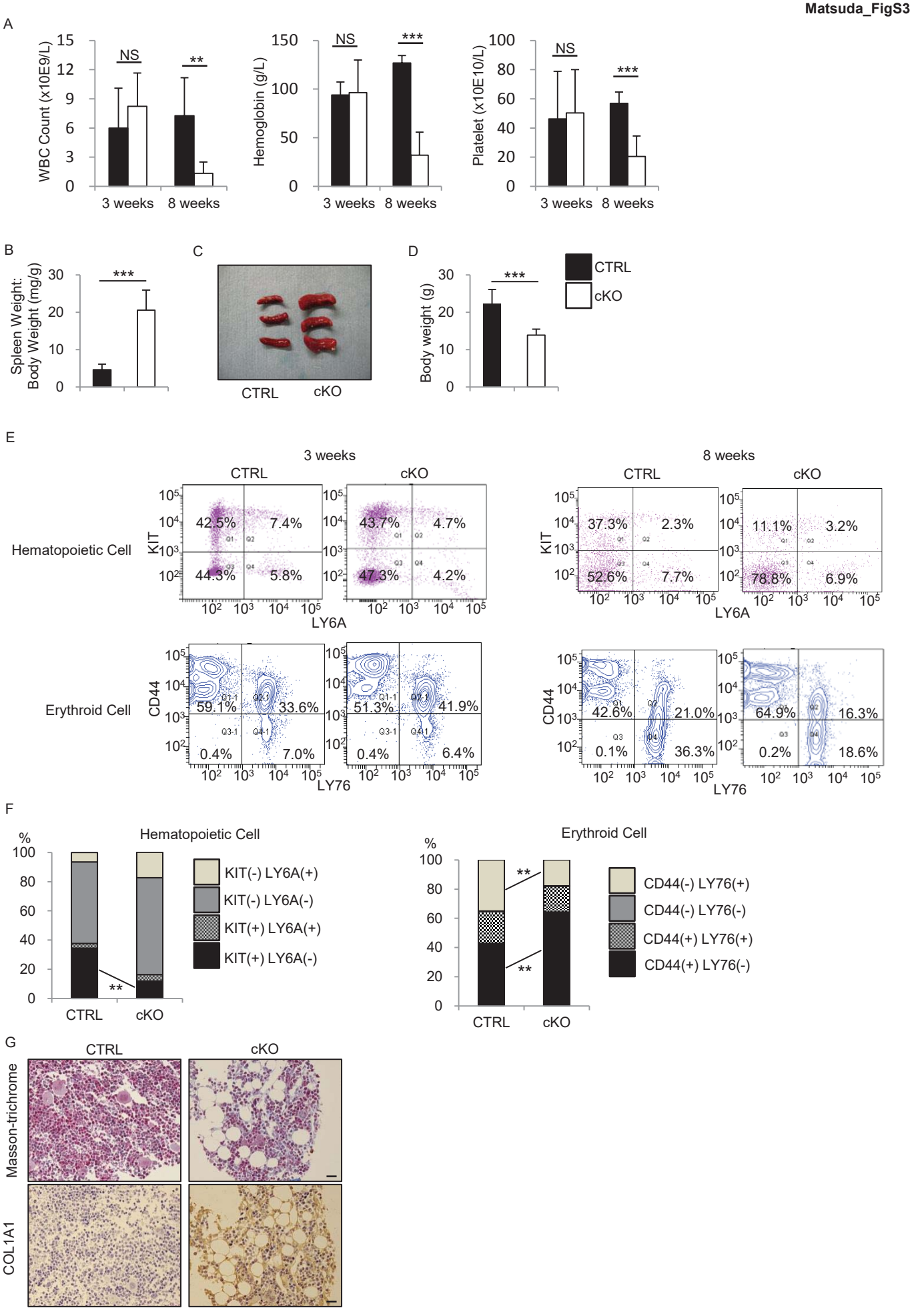
A
WBC Count (x10E9/L)
NS
**
3 weeks
8 weeks
Hemoglobin (g/L)
NS
***
Platelet (x10E10/L)
NS
***
B
Spleen Weight: Body Weight (mg/g)
***
C
CTRL
cKO
D
Body weight (g)
***
CTRL
cKO
E
3 weeks
8 weeks
CTRL
cKO
Hematopoietic Cell
KIT
LY6A
42.5%
7.4%
44.3%
5.8%
43.7%
4.7%
47.3%
4.2%
37.3%
2.3%
52.6%
7.7%
11.1%
3.2%
78.8%
6.9%
Erythroid Cell
CD44
LY76
59.1%
33.6%
0.4%
7.0%
51.3%
41.9%
0.4%
6.4%
42.6%
21.0%
0.1%
36.3%
64.9%
16.3%
0.2%
18.6%
F
Hematopoietic Cell
%
KIT(-) LY6A(+)
KIT(-) LY6A(-)
KIT(+) LY6A(+)
KIT(+) LY6A(-)
**
CTRL
cKO
Erythroid Cell
CD44(-) LY76(+)
CD44(-) LY76(-)
CD44(+) LY76(+)
CD44(+) LY76(-)
G
CTRL
cKO
Masson-trichrome
COL1A1

Figure S3. Hematopoietic abnormalities in *atg5*-cKO mice. (**A**) Peripheral blood cell counts, (**B**) the ratio of spleen (mg) to body weight (g), (**C**) representative image of spleen, and (**D**) body weight (g) of 3- (**A**) and 8- (**A** to **D**) week-old *atg5*-cKO mice and their *Atg5*-CTRL littermates. (**E**) BM cells from 3- and 8-week-old *atg5*-cKO mice and their *Atg5*-CTRL littermates were stained with the indicated antibodies and analyzed by flow cytometry. Representative plots of hematopoietic (upper) and erythroid (lower) cells. (**F**) Mean percentages of hematopoietic and erythroid progenitor cells at each developmental stage in 8-week-old mice. (**G**) Representative images of Masson trichrome- and COL1A1- staining in BM of 8-week-old *atg5*-cKO mice and their *Atg5*-CTRL littermates. n = 14 or 15 for 3-week-old mice; n = 5 to 8 for 8-week-old mice. Data are provided as the mean ± SD. NS, not significant. Statistically significant differences (***P* < 0.01, ****P* < 0.001 versus the *Atg5*-CTRL mice) are indicated. Bar: 20 μm.

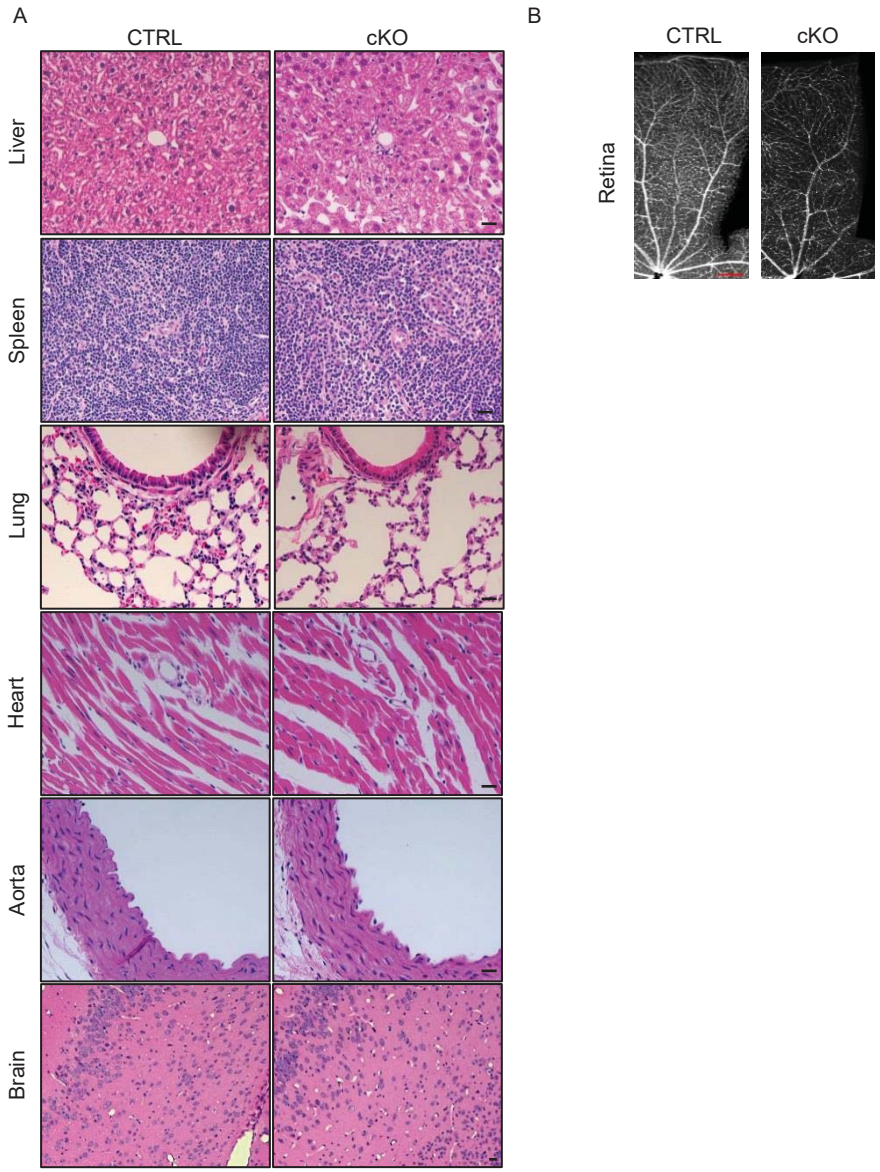

Figure S4. Endothelial-specific autophagy deficiency has no apparent impact on the organ vasculature, except in kidney. (**A**) Representative HE staining images of liver, spleen, lung, heart, aorta, and brain sections from 8-week-old *Atg5*-CTRL (left) and *atg5*-cKO (right) mice. (**B**) Representative images of immunofluorescence analysis for PECAM1 using retina from 8-week-old *Atg5*-CTRL (left) and *atg5*-cKO (right) mice. Bars: 20 μm (**A**) and 200 μm (**B**).

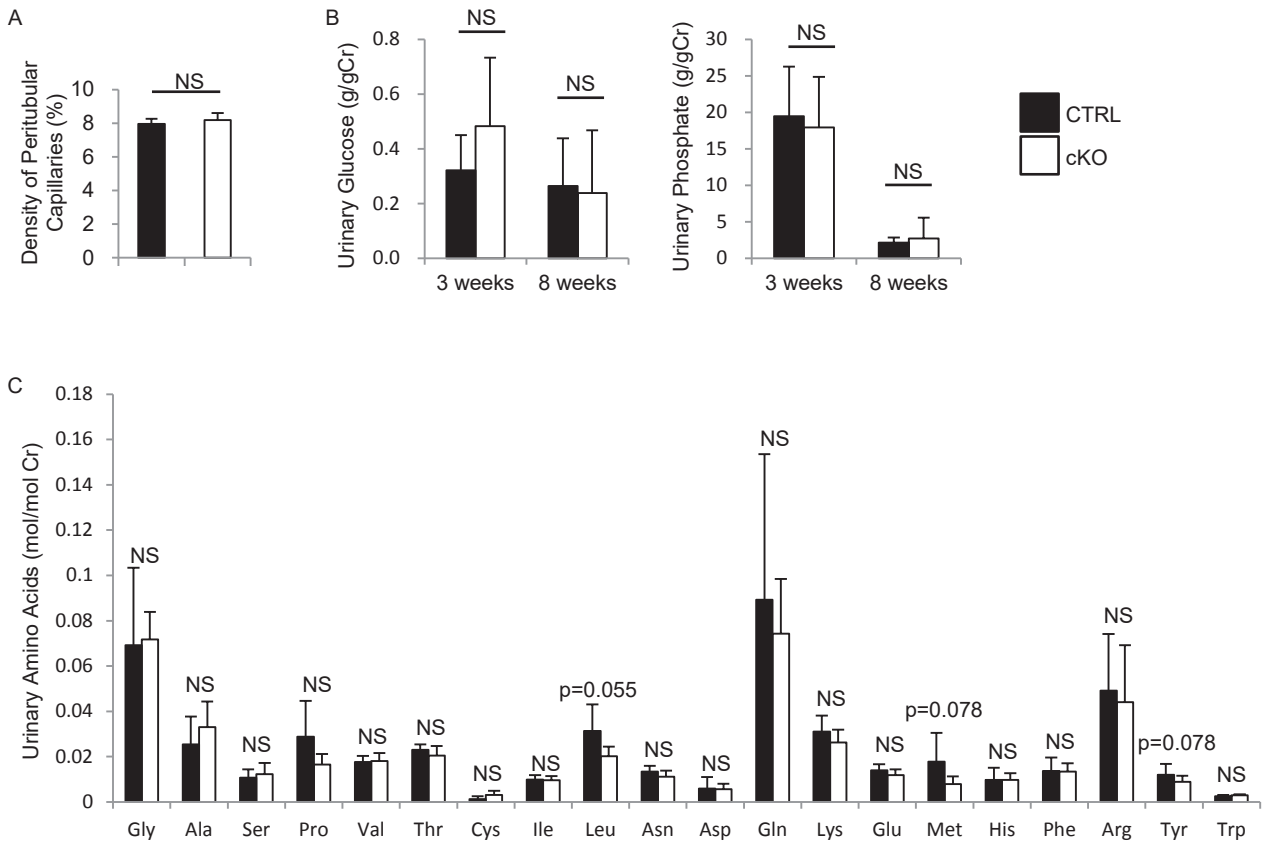

Figure S5. Effects of autophagy deficiency in the ECs on the peritubular capillaries and tubular functions. The effects of autophagy deficiency in the ECs on the peritubular capillaries and tubular functions were analyzed. The density of peritubular capillaries (**A**), the ratios of urinary concentrations of glucose, phosphate (**B**) and amino acids (**C**) to creatinine of 3- (**B**) or 8- (**A** to **C**) week-old *atg5*-cKO and *Atg5*-CTRL mice are shown. n = 4 or 5 (**A**); 5 to 8 (**B**); and 6 (**C**) in each group. Data are provided as the mean ± SD. NS, not significant.

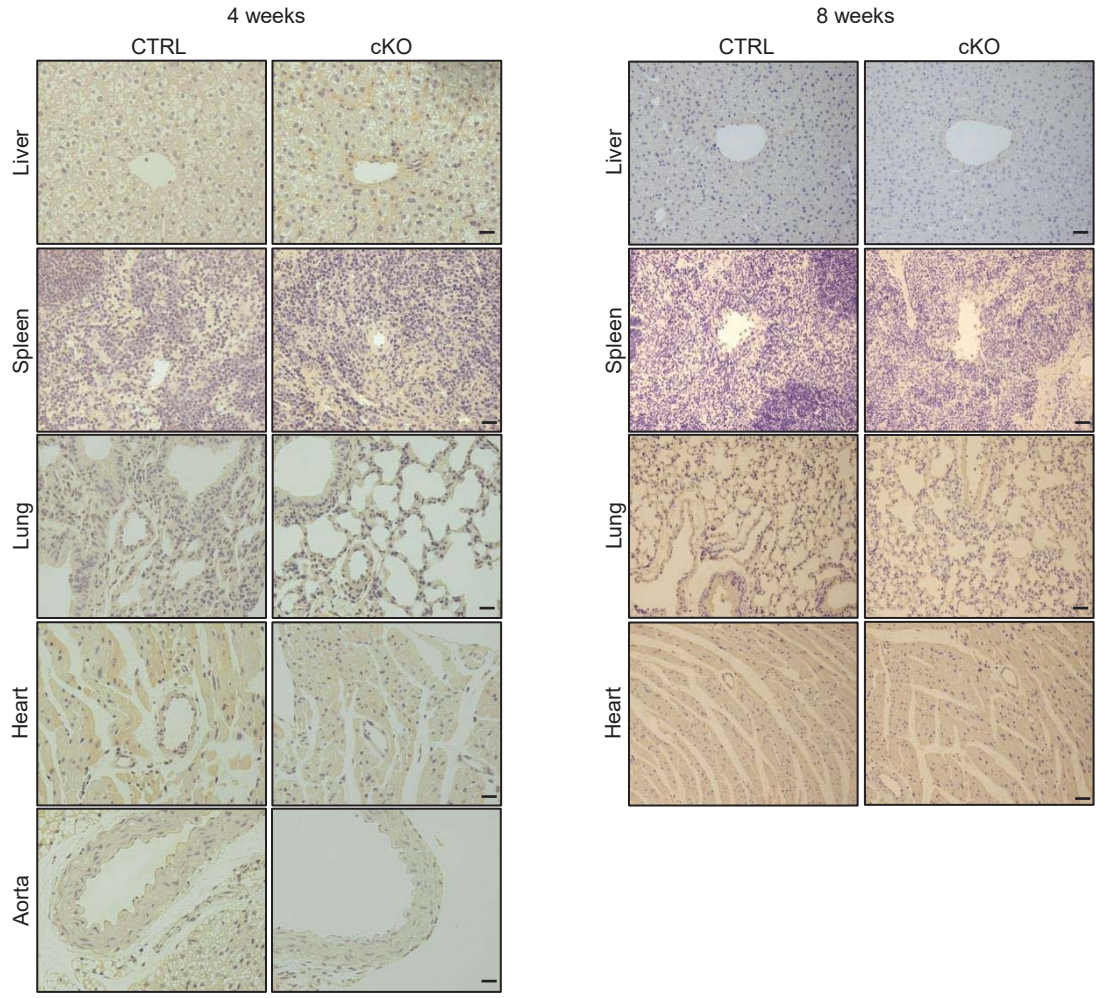

Figure S6. Absence of ROS accumulation in various organs of *atg5*-cKO mice. Representative images of immunostaining for dityrosine in sections of liver, spleen, lung, heart, and aorta from 4- and 8-week-old *Atg5*-CTRL (left) and *atg5*-cKO (right) mice. Bars: 20 μm.

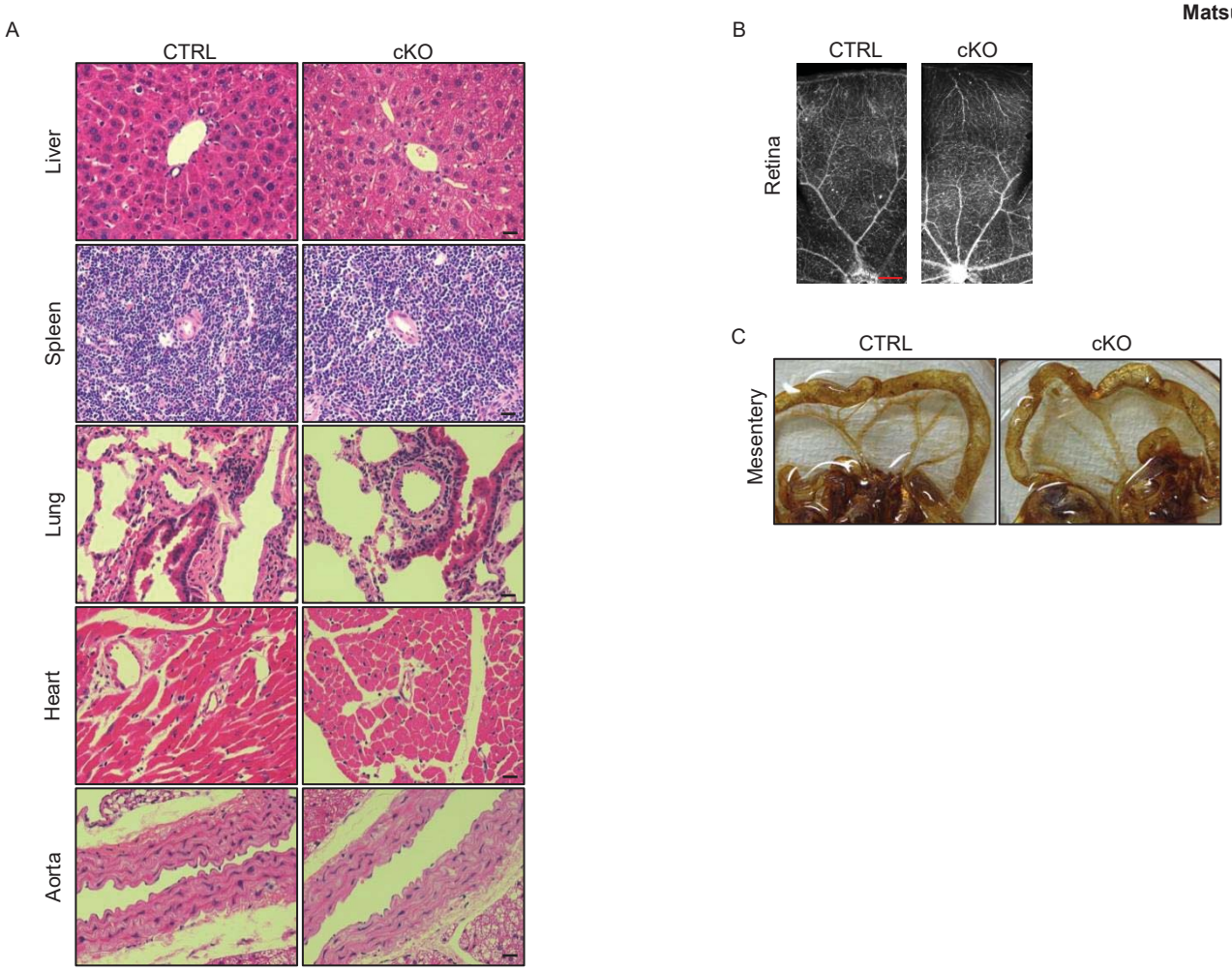

Figure S7. No obvious histological changes were detected in *atg5*-cKO recipients except in kidney. (**A**) Representative HE staining images of sections of liver, spleen, lung, heart, and aorta from 12-month-old *Atg5*-CTRL (left) and *atg5*-cKO (right) mice rescued by BMT at 4 weeks of age (*Atg5*-CTRL recipients and *atg5*-cKO recipients, respectively). (**B** and **C**) Representative images of immunohistochemical analysis for PECAM1 using retina (**B**) and mesentery (**C**) from 12-month-old *Atg5*-CTRL recipients (left) and *atg5*-cKO recipients (right). Bars: 20 μm (**A**) and 200 μm (**B**).

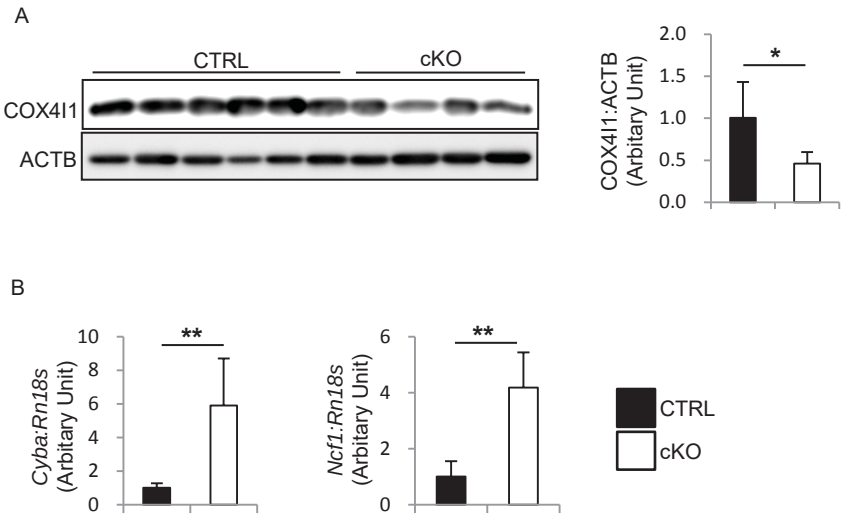

Figure S8. Effects of autophagy deficiency in the ECs on the mitochondrial function and NOX activity. The effects of autophagy deficiency in the ECs on the mitochondrial function and NOX activity were analyzed. The expression of mitochondrial protein COX4I1 (**A**) and mRNA of *Cyba* and *Ncf1*, the components of NOX, in the glomeruli of 8-week-old *atg5*-cKO and *Atg5*-CTRL mice were analyzed. n = 4 to 6 (**A**); and 8 or 9 (**B**) in each group. Data are provided as the mean ± SD. Statistically significant differences (**P* < 0.05, ***P* < 0.01 versus the *Atg5*-CTRL mice) are indicated.

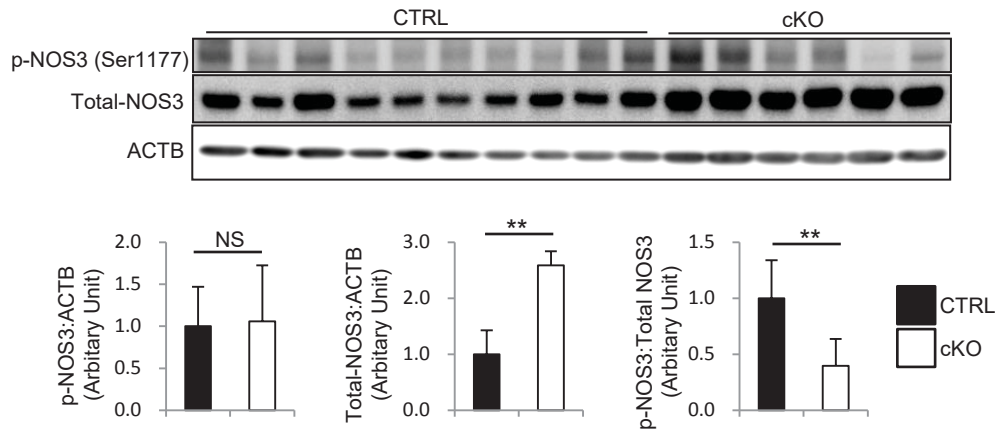

Figure S9. NOS3 inactivation in the glomeruli of *atg5*-cKO mice. The representative images of western blot analysis for p-NOS3 (Ser1177) and total NOS3 in isolated glomeruli of 8-week-old *atg5*-cKO and *Atg5*-CTRL mice. Densitometric data for p-NOS3 (Ser1177), total NOS3, and the ratio of p-NOS3 (Ser1177) to total NOS3 are shown. Data are provided as the mean ± SD. NS, not significant. Statistically significant differences (**$P < 0.01$ versus the *Atg5*-CTRL mice) are indicated.

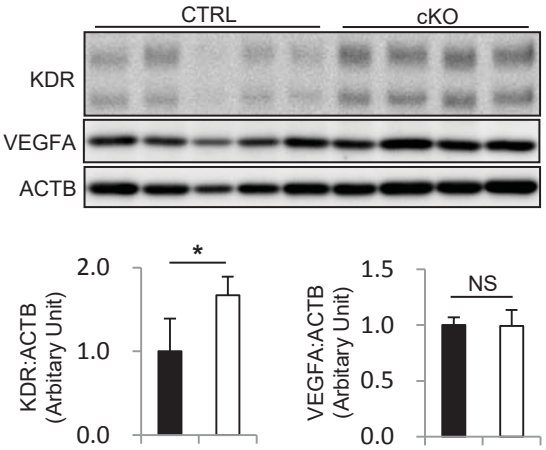

Figure S10. The VEGFA-KDR pathway may be activated in the glomeruli of *atg5*-cKO mice. The protein levels of VEGFA and KDR in the isolated glomeruli of 8-week-old *atg5*-cKO and *Atg5*-CTRL mice were analyzed by western blot analysis. Densitometric data is shown in the lower panel. n = 4 or 5 in each group. Data are provided as the mean ± SD. NS, not significant. Statistically significant differences (**P* < 0.05 versus the *Atg5*-CTRL mice) are indicated.